Supplementary Materials for

TREM2 acts as a receptor for IL-34 to suppress acute myeloid leukemia in mice

Xiaoling Xie[1,3,5], Wuju Zhang[2,3,5], Min Xiao[3,5], Tiantian Wei[3], Yingqi Qiu[1], Jingyang Qiu[3], Hao Wang[1], Zeyou Qiu[3], Sheng Zhang[3], Yating Pan[3], Linlin Mao[3], Yuhua Li[1], Bin Guo[3], Wanwen Yang[3], Yuxing Hu[1], Shujie Hu[3], Yan Gong[3], Jun Yang[3], Guozhi Xiao[4,*], Yue Zhang[3,*] and Xiaochun Bai[3,6,*]

[1]Department of Hematology, Zhujiang Hospital, Southern Medical University, Guangzhou, 510280, China

[2]Central Laboratory, The Fifth Affiliated Hospital, Southern Medical University, Guangzhou, 510910, China

[3]Guangdong Provincial Key Laboratory of Bone and Joint Degenerative Diseases, Department of Cell Biology, School of Basic Medical Sciences, Southern Medical University, Guangzhou, 510515, China

[4]Guangdong Provincial Key Laboratory of Cell Microenvironment and Disease Research, Shenzhen Key Laboratory of Cell Microenvironment and School of Medicine, Southern University of Science and Technology, Shenzhen, 518055, China

[5]These authors contributed equally

[6]Lead Contact

***Correspondence:** baixc15@smu.edu.cn (X.B.),
yugi@smu.edu.cn (Y.Z.),
xiaogz@sustech.edu.cn (G.X.)

The PDF file includes:

Fig. S1 to S13

Table S1 to S6

Supplemental Methods

In vivo animal studies

All animal studies were conducted in compliance with the protocols of the Southern Medical University Animal Care and Use Committee. Animals were housed in a pathogen-free animal facility and fed with irradiated food and sterile water. Cathepsin K (Ctsk) <tm1(cre)Ska> mice were a generous gift from Professor Shigeaki Kato (University of Tokyo), Tsc1^{tm1Djk}/J (Tsc1$^{fl/fl}$) and B6N.FVB-Tg (DMP1-cre)1Jqfe/BwdJ mice were purchased from The Jackson Laboratory (Bar Harbor, ME, USA). Tsc1$^{fl/fl}$ mice were maintained against a pure C57BL/6J background and backcrossed to C57BL/6J mice for six generations prior to use. The two independent lines of conditional Tsc1-deletion mice were generated as described previously.[1,2] DNA was isolated from partially amputated neonate tails or toes of mice for genotyping by PCR. C57BL/6 and NCG mice were used for transplantation experiments at age 6–8 weeks. Genotyping was carried out on tail DNA by PCR using specific primers as follows: Tsc1, forward: GTCACGACCGTAGGAGAAGC, reverse: GAATCAACCCCACAGAGCAT; Ctsk, common: CCTGG AAAATGCTTCTGTCCGTTTGCC, mutant: GAGTTGATAGCTGGCTG GTGGCAGATG; Dmp1, forwad: CCCGCAGAACCTGAAGATG, reverse: GACCCGGCAAAACAGGTAG. C57BL/6J-Trem2^{em2Adiuj}/J (TREM2$^{-/-}$) mice were a generous gift from Dr. Han Gao (The Third Affiliated Hospital of Sun Yat-sen University, China; JAX NO:027197), and genotyped using PCR reactions with three primers to amplify the WT and knockout alleles (TREM2, WT-reverse: AGTGCTTCAAGGCGTCATAAGT, TREM2, common: TCAGGGAGTCAGTCATTAACCA, TREM2, mutant- reverse: CAATAAGACCTGGCACAAGGA). Mouse models of C1498 (2×10^6), MLL-AF9 (2×10^5), and MV4-11 (2×10^6), as well as PDX (2×10^5) were established by transplanting leukemic cells into NOD/ShiLtJGpt-*Prkdc*^{em26Cd52}*Il2rg*^{em26Cd22}/Gpt (NCG) mice as described previously.[3-5]

Ex vivo osteoclast culture

Osteoclast-like cells were generated from non-adherent, M-CSF-dependent bone marrow cells. The BM cells were isolated from $Tsc1^{Ctsk}$ mice and control mice, washed twice, suspended (10^5 cells/mL) in MEM supplemented with 5 ng/mL M-CSF (Peprotech, Rocky Hill, CA, USA), and incubated for 24 h. Non-adherent cells were then collected by centrifugation and resuspended (10^5 cells/mL) in MEM containing M-CSF (20 ng/mL) and RANKL (50 ng/mL) to induce osteoclastogenesis. Cultures were fed every 3 days by replacing fresh medium. Cultures were maintained for 8–10 days. The osteoclasts were then evaluated using tartrate-resistant acid phosphatase (TRAP) staining.

Ex vivo BMDM culture

For primary BMDM culture, bone marrows of tibiae and femurs from 10 weeks C57BL/6J or $TREM2^{-/-}$ mice were flushed with PBS. Cells were resuspended and filtered through 70 μm nylon sieves. Erythrocytes were lysed with red blood cell lysis buffer. Cells were cultured in DMEM media supplemented with 10% fetal bovine serum (FBS), 1% penicillin/streptomycin, and 10 ng/mL M-CSF for 5–7 days.

Cell lines

MV4-11, NB4, KG-1, THP-1, and HEK 293T cells were cultured in RPMI-1640 (Invitrogen, Carlsbad, CA, USA) supplemented with 10% FBS and 1% penicillin/streptomycin (Invitrogen) at 37°C with 5% CO_2. C1498 cells were kept in our laboratory and grown in DMEM (Thermo Fisher Scientific, Waltham, MA, USA) with 10% FBS and 1% penicillin/streptomycin. All cell lines were acquired from the American Type Culture Collection or Deutsche SammLung von Mikroorganismen und Zellkulturen. Murine MLL-AF9 blasts were kindly provided by Dr. Tao Cheng[6,7] (State Key Laboratory of Experimental Hematology, National Clinical Research Center for Hematological Diseases, Institute of Hematology and Blood Diseases Hospital, Chinese Academy of Medical Sciences and Peking Union Medical College) and were maintained in Iscove's Modified Dulbecco's Medium (IMDM; Thermo

Fisher Scientific) supplemented with 15% FBS and murine (m) stem cell factor (SCF) (50 ng/mL), mIL-3 (20 ng/mL), and mIL-6 (10 ng/mL). All cells were tested regularly for mycoplasma using a commercially available kit (MycoAlert mycoplasma detection kit; Lonza, GA, USA) and were authenticated using short tandem repeat profiling.

Primary cell culture

$CD34^+$ BM mononuclear cells from human BM aspirates were obtained by Ficoll-Paque density gradient centrifugation and a CD34 MicroBead Kit (Miltenyi Biotec, Auburn, CA, USA) following the manufacturer's instructions. Isolated cells were verified by fluorescence-activated cell sorting to >95% purity. All primary cells were kept in IMDM supplemented with 20% FBS, human (h) IL-3 (10 ng/mL), hSCF (50 ng/mL), hFLT3 ligand (50 ng/mL), human granulocyte-colony-stimulating factor (10 ng/mL), thrombopoietin (25 ng/mL), and hIL-6 (20 ng/mL) (Peprotech).

Generation of IL-34-KO mice

The IL-34 (embryonic KO)/B6 mouse model with a C57BL/6J background was created in our laboratory. Briefly, four guide RNA sequences (gRNAs) were designed to disrupt early exon 3 according to the off-target scores (http://www.genome-engineering.org; IL-34 gRNA: CAGGTGCATGCAGAGCCCTAAGG), transcribed using a MEGAshortscript T7 kit (Thermo Fisher Scientific), and then purified using a MEGAclear Kit (Thermo Fisher Scientific). Cas9 mRNA was in vitro transcribed using a mMESSAGE mMACHINE T7 ULTRA kit (Thermo Fisher Scientific). Approximately 1 nL of Cas9 mRNA and gRNA mixture was injected into the cytoplasm of one-cell-stage C57BL/6J embryos. The injected embryos were transferred immediately into the oviductal ampulla in pseudopregnant CD-1 Fs. Four mice tested positive for the excised allele and were heterozygous for the constitutive allele ($IL\text{-}34^{+/-}$). These mice were analyzed by Sanger sequencing and backcrossed with C57BL/6J mice for more than six generations, and then used for further breeding to establish stable ($IL\text{-}34^{-/-}$) mice.

Cell viability and clonogenic assays

For cell viability analysis, cells were seeded in 96-well plates at a density of 2×10^3 per well and treated with increasing concentrations of IL-34 (0–200 ng/mL). The relative viabilities of cell cultures after treatment for 48 h were assessed using CellTiter-Glo Luminescent Cell viability assay kits (Promega). For colony-forming unit assays, cells were seeded in 24-well plates in methylcellulose medium (MethoCult H4434; StemCell Technologies). Colonies were counted and photographed under a microscope (Zeiss, Jena, Germany) after 2 weeks of incubation.

Immunoblotting

Lysates were prepared from total cellular protein pellets extracted using lysis buffer (Absin, China) containing protease inhibitor cocktail (Roche), and subjected to western blot using specific antibodies for Rasal3 (Immunoway, 1:500), phosphorylated (p)-MAP4K1 (Bioss, 1:1,000), MAP4K1 (Cell Signaling Technology, 1:1,000), ERK1/2 (Cell Signaling Technology, 1:1,000), c-Myc (Cell Signaling Technology, 1:1,000), phospho-Ser/Thr-Pro (Cell Signaling Technology, 1:1,000), and p-ERK1/2 (T202/Y204, Cell Signaling Technology, 1:1,000). The relative protein band intensity was normalized against a loading control (glyceraldehyde 3-phosphate dehydrogenase, GAPDH) and compared to the relative control. Antibodies were listed in **Table S5**.

Cell differentiation assay

Cultured cells or primary murine cells were stained with CD11b or Gr-1 antibodies. GFP^+ or GFP^- populations were gated for standard flow cytometry analysis to detect CD11b and Gr-1 expression levels. Cultured cells were also processed with standard May-Grünwald Giemsa staining.

Identification and quantification of IL-34 target proteins using SPR and HPLC-MS

The three-dimensional Photo-cross-linker Sensor CHIP™ (Betterways Inc., China) can immobilize IL-34 without chemical label linking. For spotting, IL-34 and control samples were produced on the chip surface by auto-spotting three times using a BioDot™-1520 array printer (BIODOT Inc., CA, USA), and C1498 cell lysate was used as the liquid phase. The H2 sample curve signal indicated target protein binding on the area spotted with IL-34, and the background curve indicated the change in the signal in the non-spotted area. The timing of the procedures was as follows: the system was pre-washed to infiltrate the surface of the chip with running buffer at 0–260 s (resonance intensity about 0 resonance units (RU); binding began at 260–520 s, with IL-34 on the chip surface starting to capture the protein targets in the cell lysate; the chip was washed at 520–820 s to gradually remove non-bound and non-specific molecules, while the target protein that bound specifically to IL-34 remained on the chip surface; resonance intensity decreased until it reached a plateau at ~542.65 RU; and the background resonance intensity gradually decreased to baseline (~37.72 RU) as non-specific binding to the non-spotted areas gradually decreased, i.e., the chip background noise returned to the normal level.

SPRi

IL-34 was bound to an optical biosensor chip and protein samples were injected into the chip at a rate of 2 μL/s at 25°C. Oval regions of interest (ROIs) in the imaging area were automatically set using the data-collection software. The ROIs of rapamycin and dimethylsulfoxide were used as positive and negative controls, respectively. The protein samples were diluted in PBS (pH 7.4) containing 0.05% Tween-20 and then used as analytes with an association and dissociation at a 2 μL/s flow rate of different concentrations by serial dilution. A regeneration injection of glycine-HCl (pH 2.0) was used to remove bound proteins, and the chips were reusable for further experiments.

Homology modeling

ProMod3 extracts structural information from an aligned template structure by

transferring conserved atom coordinates defined by the target template alignment. Residue coordinates corresponding to insertions/deletions in the alignment are then generated by loop modeling and a full-atom protein model is obtained by constructing the non-conserved amino acid side chains. Final candidates are then selected using statistical potentials of mean force scoring methods. If no suitable fragments can be found, a conformational space search is performed using Monte Carlo sampling. Non-conserved side chains are modeled using the 2010 backbone-dependent rotamer library provided by the Dunbrack Lab.[8] ProMod3 implements the SCWRL4 energy function to estimate pairwise energies between rotamers and towards parts of the protein model by minimizing the overall energy. Additionally, ProMod3 implements the graph-based TreePack algorithm. Finally, small structural distortions, unfavorable interactions, or clashes introduced during the modeling process are resolved by energy minimization. ProMod3 uses the OpenMM library to perform the computations and the CHARMM27 force field for parameterization. The amino acid sequence of TREM2 was retrieved from the UniProtKB database (Protein ID: 6B8O) and subjected to BlastP against the PDB database to identify the templates. The sequence identity was 74.34%.

Protein-protein docking

To obtain insights into the interactions between IL-34 and TREM2, we submitted the two proteins to the ClusPro[9] protein-protein docking server. The crystal structure of IL-34 was downloaded from the Protein Data Bank, and PDB 4EXP was used for docking. We first set IL-34 as the ligand and TREM2 as the receptor for protein docking. IL-34 was then rotated with 70,000 rotations to perform docking simulations with the rigid receptor. The translation with the best score was chosen from each rotation. Of the 70,000 rotations, we chose the 1,000 rotation/translation combinations with the lowest scores. The ClusPro docking server then clustered 1000 GAG positions with the lowest energy scores within a 9 Å interface root-mean-square deviation cut-off and the 10 best-scored cluster centers with the most cluster members were then retrieved and inspected visually one by one. The intermolecular contacts

from the most probable poses were further evaluated. The interacting residues of the representative models from the largest clusters were analyzed by Molecular Operating Environment software (Chemical Computing Group). PyMOL (Schrödinger) was used to generate molecular graphics.

Plasmid constructions and recombinant protein expression

The full-length His-tagged mouse TREM2 cDNA and GST-tagged mouse IL-34 cDNA were purchased from VectorBuilder (Guangzhou, China). IL-34 was constructed into the pET16b-BsaI-ccdB-Cm-BsaI vector, fused with GST tags. TREM2 was constructed into the pET16b-6xHis-BsaI-ccdB-Cm-BsaI vector. All constructs were verified by DNA sequencing analysis. The vectors were transformed into Escherichia coli BL21 and the proteins expressed as GST fusion or His fusion proteins. The GST-IL-34 fusion protein was affinity-purified by using glutathione-Sepharose beads (G4551, Sigma) and a batch method.[10] The His-TREM2 fusion protein was purified by immobilized metal chelate affinity chromatography on Ni-NTA beads as described previously.[11]

Immunoprecipitation and GST pull-down

Cells were lysed in 1 × IP lysis buffer (Thermo Fisher Scientific). Immunoprecipitation was performed by incubation with an anti-TREM2 antibody (Cell Signaling Technology) or anti-IL-34 antibody (Abcam) at 4°C overnight, followed by incubation with Protein A/G Plus-Agarose (GE Healthcare) at 4°C for 2 h with gentle rotation. The beads were washed three times with 1 × IP lysis buffer followed by boiling for 15 min in reducing sodium dodecyl sulfate (SDS) sample buffer. The immunoprecipitated proteins were separated on an SDS-polyacrylamide gel and immunoblotted with corresponding antibodies. For GST pull-down assay, GST or GST-TREM2 fusion proteins were immobilized on GST beads and incubated with His-tagged IL-34 binding buffer. The expression of GST fusion proteins was confirmed by SDS-polyacrylamide gel electrophoresis and Coomassie Blue staining. The interaction of His-TREM2 and GST-IL-34 was confirmed by immunoblotting, as

described above.

Knockout of CSF1R, PTPRZ1, SDC1, and TREM2 using CRISPR/Cas9-mediated genome editing

Stable CSF1R-, PTPRZ1-, SDC1-, and TREM2-KO C1498 cell lines were generated using the Cas9/guide RNA ribonucleoprotein complex (Cas9/RNP) delivered directly to the cells by electroporation. C1498 cells were electroporated using the Neon transfection system (Thermo Fisher Scientific). C1498 cells were assessed for cleavage efficiency and evaluated for viability 4 days after transfection. Sequence analysis was then performed to confirm the presence of intact CRISPR targets in C1498 cells. CRISPR guide RNA sequences were designed using the *http://crispr.mit.edu* web site (TREM2 gRNA: 5'-TCAGCAGCAGGAGAAACTGG-3'; CSF1R gRNA: 5'-TTCAAGCTCGGTACA ACGGTAGG-3'; PTPRZ1 gRNA: 5'-ACAGGAGCTGAACGCACGCGAGG-3'; SDC1 gRNA: 5'- TCCTCGGGCTTCTCTCCGGCTGG-3'). Using a 10 μL tip, C1498 cells were transfected with 200 ng of gRNA, 1 μg of GeneArt® Platinum™ Cas9, and 10 pmol of single-stranded oligos using the Neon® Transfection System Kit (Thermo Fisher Scientific). Stable KO generations with the highest cleaving efficiency were expanded, harvested, and sorted, and single cells were then distributed into 96-well plates and single growing colonies were consolidated and replated. To determine the presence of insertions or deletions (indels) in targeted clones, genomic DNA was isolated using a Quick-DNA Miniprep kit (Zymo Research) and PCR amplification was carried out using 2× Taq Master Mix (Dye Plus; Vazyme, P112) with primers flanking the exon. Plasmids were isolated from 8–10 single colonies and sequenced by Sanger sequencing (Genewiz, China). Clones with mutations in both alleles were selected for downstream studies. Cell lines generated using the above strategy included gene (+/+), (+/-), (+/-A), (+/−B), and (-/-) cells. All clones were maintained under the same conditions as the parental cells.

Viral vector production and cell transduction

Stable knockdown of TREM2 was achieved by infection of THP-1 cells with commercially available lentiviral particles and scrambled controls. The constitutively active mutant of MAPK1/2 was designed by substitution of the regulatory phosphorylation sites Tyr185 and Thr204 with aspartic acid (Y185D/T204D mutant). Viruses were produced by transfecting 293T cells using Lipofectamine 3000 (Thermo Fisher Scientific) and collected 48–72 h following transfection, filtered through a 0.45 μm low protein-binding membrane (Millipore), and then concentrated by centrifugation at 2,000 r.p.m. for 10 min. C1498, THP-1, and MV4-11 cells were infected with viral supernatants supplemented with 8 μg/mL Polybrene (Sigma-Aldrich). At 72 h after infection, stably transduced cells were sort-purified using a FACSAria III (BD Biosciences, San Diego, CA, USA) to give a homogeneous population of GFP-labeled cells.

RNA sequencing assay

C1498 cells were treated with murine IL-34 (R&D System, USA, 100 ng/mL) for 30 min, and total RNA was isolated and extracted. Libraries were constructed and 150 bp paired-end sequencing was carried out using an Illumina Novaseq platform (Illumina). Quality control of the sequencing data was performed by mapping reads to the reference genome and by quantification of gene expression levels and differential expression analysis. Downstream analysis included differential expression analysis, GO terms, and KEGG pathway enrichment. Genes for which the expression differed by more than 2-fold in the IL-34-treated groups compared with control groups were identified. Differential gene expression between samples was determined using the R package DEGseq, and adjusted *P* values were calculated using the Benjamini-Hochberg method. A q-value < 0.05 was considered significant.

Phosphoproteomics

For protein extraction, C1498 cells treated with murine IL-34 or control were subjected to global quantitative phosphoproteomics analysis (PTM Bio, China). Cells

were washed twice with ice-cold PBS and ruptured with lysis buffer (Pierce, Rockford, IL, USA) containing cocktail proteinase inhibitors and phosphatase inhibitor cocktail (Roche). Whole protein extracts were centrifuged at 12,000 × *g* at 4°C for 10 min, the supernatants were collected, and the protein concentration was quantified by the BCA protein assay (Thermo Fisher Scientific). For enzymatic digestion, the protein solution was reduced with 5 mM dithiothreitol for 30 min at 56°C and alkylated with 11 mM iodoacetamide for 15 min at 37°C using an enzyme:substrate ratio of 1:50 (w/w). Digested lysates were then centrifuged to remove the precipitate. The resulting peptides were desalted using a 500 mg C18 cartridge and dried *in vacuo*. Phosphopeptide enrichment was carried out using prepacked TiO_2 tips. Phosphorylated peptides were enriched using Fe(III)-NTA cartridges (Agilent Technologies) in an automated fashion using the AssayMAP Bravo Platform (Agilent Technologies), and dried using a SpeedVac concentrator (Thermo Fisher Scientific). For MS-based phosphopeptide analysis, peptides were subjected to nanoscale liquid chromatography-tandem mass spectrometry using an UltiMate (Thermo Fisher Scientific) coupled online to the ultra-HPLC system. Instruments were operated in data-dependent mode of one MS scan followed by 20 MS/MS scans. For data analysis, the resulting mass spectra were searched using MaxQuant (v.1.5.2.8) and the UniProt Human databases using the SEQUEST algorithm. The false discovery rate for peptides, proteins, and site identification was set to 1%.

Monitoring and flow cytometry analysis

PB counts were examined by standard methodology using an automated blood cell counter (Scil Animal Care Company). Blood smears and purified BM and spleen cells were centrifuged at 800 r.p.m for 5 min on slides (2×10^5 cells/slide). Pieces of the spleen and liver were fixed in 4% paraformaldehyde and stored. For flow cytometry, red blood cells and BM cells were lysed with red cell lysis buffer on ice (Solarbio, China), and stained at 4°C for 25 min with the following antibodies: human CD45-allophycocyanin (APC) (BioLegend, San Diego, CA, USA), mouse F4/80 (BioLegend), mouse CD45-phycoerythrin (BioLegend), human/mouse CD11b-APC

(BioLegend), mouse Ly-6G/Ly-6C (Gr-1)-fluorescein isothiocyanate (FITC) (BioLegend), and DAPI (Biolegend). Analysis was performed using a CytoFLEX 3 (Beckman Coulter, Pasadena, CA, USA).

Intracellular staining

Human primary cells were labeled with human CD45-APC and human CD33/CD34-FITC antibodies *in vitro* at 4°C for 30 min. Intracellular staining of TREM2 (Biolegend) was performed using a Fix and Perm kit (eBioscience). Briefly, cells were washed with chilled PBS, fixed with 4% paraformaldehyde at 4°C for 30 min, permeabilized with permeabilization buffer, and incubated with rabbit anti-human TREM2-APC for 30 min at room temperature in the dark. Stained cells were washed with chilled PBS and resuspended in PBS for flow cytometry.

Immunofluorescence staining and confocal microscopy

C1498 cells were spun onto slides using a cytospin centrifuge after IL-34 treatment, fixed with 4% paraformaldehyde for 20 min, permeabilized with 0.1% Triton X-100 for 15 min, blocked with 5% bovine serum albumin for 30 min at 37°C, and then stained with primary antibodies (TREM2 and IL-34). After incubation, cells were washed and stained with fluorochrome-conjugated secondary antibody (Molecular probes) for 1 h at room temperature (RT). The nuclei were stained with 4′,6-diamidino-2-phenylindole (DAPI) solution (5 μg/mL). Images were taken under a confocal laser-scanning microscope (Leica).

Quantitative RNA expression assays

Total RNA was extracted from cells using an RNAeasy Plus Mini Kit (Qiagen) and cDNA was synthesized using a SuperScript VILO cDNA Synthesis Kit (Invitrogen). Quantitative real-time PCR reactions were carried out using SYBR Premix Ex Taq (TaKaRa Bio USA, Mountain View, CA, USA) in an ABI 7500 system (Applied Biosystems, Foster City, CA, USA). The $2^{-\Delta\Delta Ct}$ method was used to normalize the relative expression levels of the target genes. The specific sequences of primers used

for qPCR analysis are listed: mIL-34 (forward: 5'-TTGCTGTAAACAAAGCCCCAT-3', reverse: 5′-CCGAGACAAAGGGTACACA TTT); hTRME2 (forward: 5′-TCAATCCAGGAGCACAGTTCC-3', reverse: 5′-CCACTCAACGCAGATGCAGC-3'). All primer sequences were listed in **Table S6**.

Histology and immunohistochemistry

Tissues were fixed in 4% paraformaldehyde and embedded in paraffin. Bone tissues were decalcified prior to embedding. Following deparaffinization and heat-induced epitope unmasking, the slides were stained with anti-human CD45 (Dako, 1:100) overnight at 4°C followed by horseradish peroxidase (HRP)-conjugated IgG (ImmunoWay, USA) for 1 h. The color was then developed by incubation with a DAB Substrate kit. After washing in PBS, tissue sections were counterstained with hematoxylin and photographed under conventional light-field microscopy using an optical microscope (Olympus, Japan).

ELISA assay

The level of IL-34 in osteoclast culture supernatant and serum level of IL-34 in patients were measured by enzyme-linked immunosorbent assay. The assay kit for murine IL-34 (Cat No: E-EL-M0720c) was purchased from Elabscience (Wuhan, China) and the kit for human IL-34 (Cat No: RK0018) was purchased from Abclonal (Wuhan, China).

Ras GTPase activation assay

Ras activity was assessed by detecting Ras-GTP in the cells by using a Ras activation assay kit (WuHan New East Biosciences Co., Ltd.) according to the manufacturer's protocol. In brief, cells (1×10^7) were treated with lysis buffer plus protease inhibitor cocktail (Roche) with gentle shaking. The lysates were then incubated with anti-Ras antibody Y13–259 (Invitrogen, specifically recognizes activated Ras) and protein A/G agarose bead at 4°C for 1 h. The precipitates were washed three times with the same

lysis buffer. The immunoprecipitates were washed and then resuspended in 2× loading buffer and heated to 100°C for 5 min to elute GTP and GDP from the immunoprecipitated Ras. The amounts of activated Ras were further determined by immunoblotting.

Statistics and reproducibility

Data were presented as mean ± standard error or mean ± standard deviation (SD) using GraphPad Prism 8. Comparisons between two groups were performed by unpaired Student's *t*-tests or one-way ANOVA. Survival curves were obtained from Kaplan–Meier estimates and validated with the log-rank test. All experiments were carried out with at least three biological replicates.

References

1. Xu S, Zhang Y, Wang J, et al. TSC1 regulates osteoclast podosome organization and bone resorption through mTORC1 and Rac1/Cdc42. Cell Death Differ. 2018;25:1549-1566.
2. Liu W, Wang Z, Yang J, et al. Osteocyte TSC1 promotes sclerostin secretion to restrain osteogenesis in mice. Open Biol. 2019;9:180262.
3. Vick B, Rothenberg M, Sandhofer N, et al. An advanced preclinical mouse model for acute myeloid leukemia using patients' cells of various genetic subgroups and in vivo bioluminescence imaging. Plos One. 2015;10:e120925.
4. Maes T, Mascaro C, Tirapu I, et al. ORY-1001, a Potent and Selective Covalent KDM1A Inhibitor, for the Treatment of Acute Leukemia. Cancer Cell. 2018;33:495-511.
5. Minzel W, Venkatachalam A, Fink A, et al. Small Molecules Co-targeting CKIalpha and the Transcriptional Kinases CDK7/9 Control AML in Preclinical Models. Cell. 2018;175:171-185.
6. Huang D, Sun G, Hao X, et al. ANGPTL2-containing small extracellular vesicles from vascular endothelial cells accelerate leukemia progression. J Clin Invest. 2021;131.
7. Gao A, Gong Y, Zhu C, et al. Bone marrow endothelial cell-derived interleukin-4 contributes to thrombocytopenia in acute myeloid leukemia. Haematologica. 2019;104:1950-1961.
8. Shapovalov MV, Dunbrack RJ. A smoothed backbone-dependent rotamer library for proteins derived from adaptive kernel density estimates and regressions. Structure. 2011;19:844-858.

9. Kozakov D, Hall DR, Xia B, et al. The ClusPro web server for protein-protein docking. Nat Protoc. 2017;12:255-278.

10. Fang N, Hu C, Sun W, et al. Identification of a novel melatonin-binding nuclear receptor: Vitamin D receptor. J Pineal Res. 2020;68:e12618.

11. Huang Y, Su R, Sheng Y, et al. Small-Molecule Targeting of Oncogenic FTO Demethylase in Acute Myeloid Leukemia. Cancer Cell. 2019;35:677-691.

Supplementary Figures

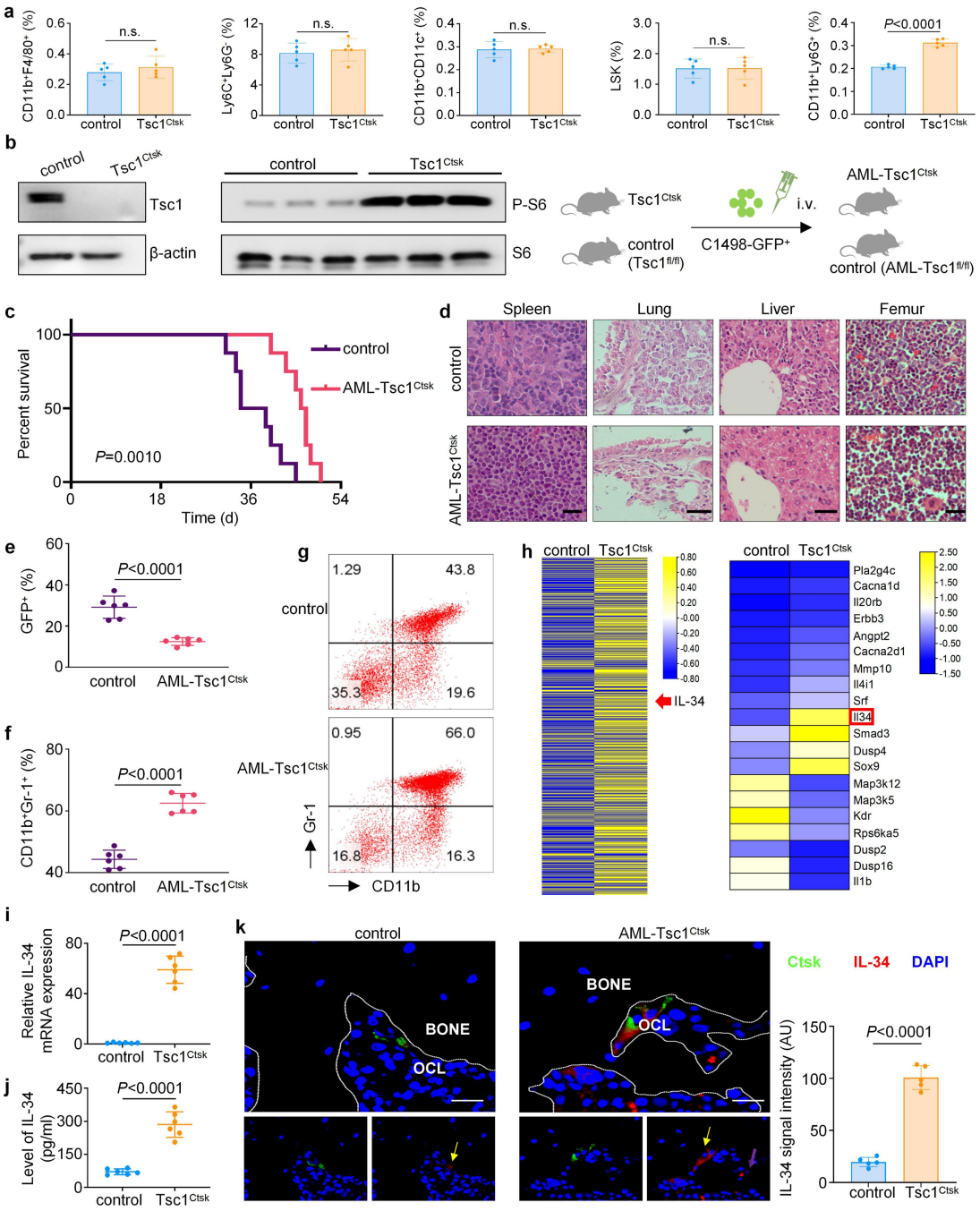

Fig. S1. Tsc1-deficient osteoclasts produced high levels of IL-34, which delayed AML progression and improved survival in Tsc1^{Ctsk} mice.

a, Flow cytometry analysis of BM monocyte-derived macrophages (CD11b$^+$F4/80$^+$), monocytes (Ly6C$^+$Ly6G$^-$), monocyte-derived dendric cells (CD11b$^+$CD11c$^+$), Lin$^-$Sca-1$^+$c-kit$^+$ (LSK) cells, and neutrophils (CD11b$^+$Ly6G$^+$) in 12-week-old Tsc1^{Ctsk} and control mice (n = 5).

b, Immunoblotting analysis of Tsc1, phospho-S6 (P-S6), and S6 levels in primary osteoclasts from $Tsc1^{Ctsk}$ mice and littermate controls (left). Experimental design (right).

c, Kaplan–Meier survival curves of $Tsc1^{Ctsk}$ mice and littermate controls engrafted with C1498-GFP^+ cells (n = 8). Statistical analysis by the log-rank (Mantel-Cox) test.

d, Representative hematoxylin and eosin (H&E)-stained tissue sections of AML-$Tsc1^{Ctsk}$ and control leukemic mice. Scale bars, 200 μm (femur and spleen); 100 μm (liver and lung).

e, Percentages of GFP^+ BM cells from AML-$Tsc1^{Ctsk}$ and control leukemic mice (n = 6).

f–g, Flow cytometry analysis of BM $CD11b^+Gr\text{-}1^+$ neutrophils in AML-$Tsc1^{Ctsk}$ and control leukemic mice (n = 6).

h, Heatmaps of differentially expressed mRNA in osteoclasts from $Tsc1^{Ctsk}$ and control mice (left), with examples of differentially expressed genes (right).

i, qPCR analysis of IL-34 levels in osteoclasts from $Tsc1^{Ctsk}$ and control mice (n = 6).

j, IL-34 levels in culture supernatant collected from Tsc1-deficient osteoclasts and control cells determined by enzyme-linked immunosorbent assay (n = 6).

k, Immunofluorescence co-staining of IL-34 (red) and Ctsk (green) in bone sections from AML-$Tsc1^{Ctsk}$ mice and control leukemic mice. Yellow arrows indicate IL-34-positive osteoclasts, and purple arrows indicate IL-34-positive red blood cells (unspecific staining). Scale bars, 50 μm. Quantification analysis was determined by the intensity of IL-34 immunostaining on the bone surface or in BM per image.

The *P* values were calculated using a 2-tailed, unpaired Student *t* test.

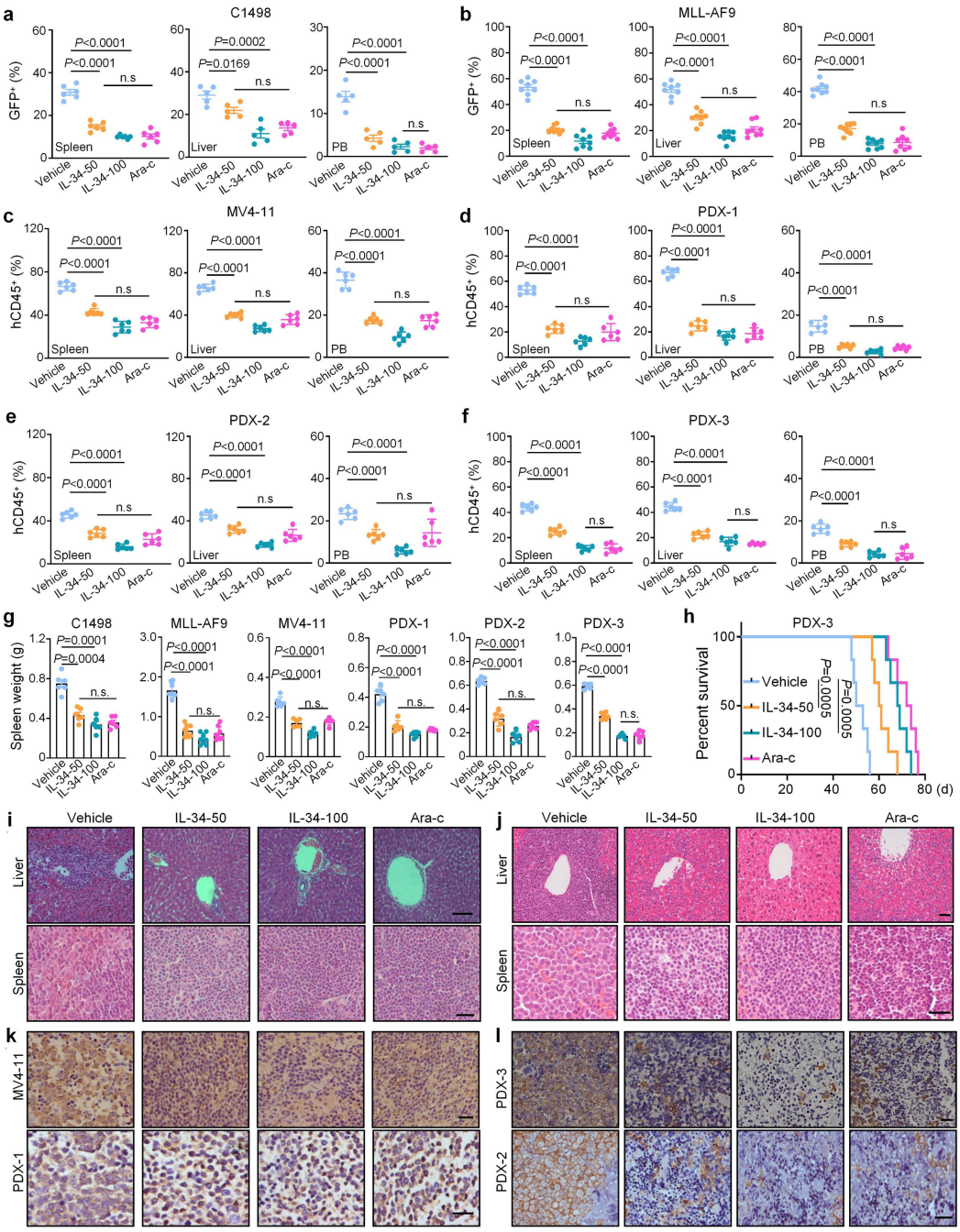

Fig. S2. IL-34 displayed therapeutic potential in multiple AML models (see also Fig. 1).

a–**f**, Percentages of AML spleen cells (left panel), liver cells (middle panel), and PB cells (right panel) from C1498-GFP (**a**), MLL-AF9-GFP (**b**), MV4-11 (**c**), and PDX (**d**–**f**) xeno-transplanted mice treated with vehicle, Ara-C, or IL-34 (50 and 100 μg/kg) (n = 6).

g, Spleen weights of mice at day 28 (n = 6).

h, Kaplan–Meier survival curves of PDX xeno-transplanted mice (n = 6) after

treatment with vehicle, IL-34 (50 μg/kg or 100 μg/kg), or Ara-C. *P* values determined by log-rank test.

i–j, H&E-stained spleen and liver from C1498-GFP (**i**) and MLL-AF9-GFP (**j**) xeno-transplanted mice treated with vehicle, Ara-C, or IL-34. Scale bars, 50 μm.

k–l, Infiltration of leukemia cells in spleen indicated by CD45 immunohistochemistry from MV4-11-bearing and primary PDX mice. Scale bars, 50 μm.

Statistical significance was calculated by one-way ANOVA with Turkey's multiple comparison test.

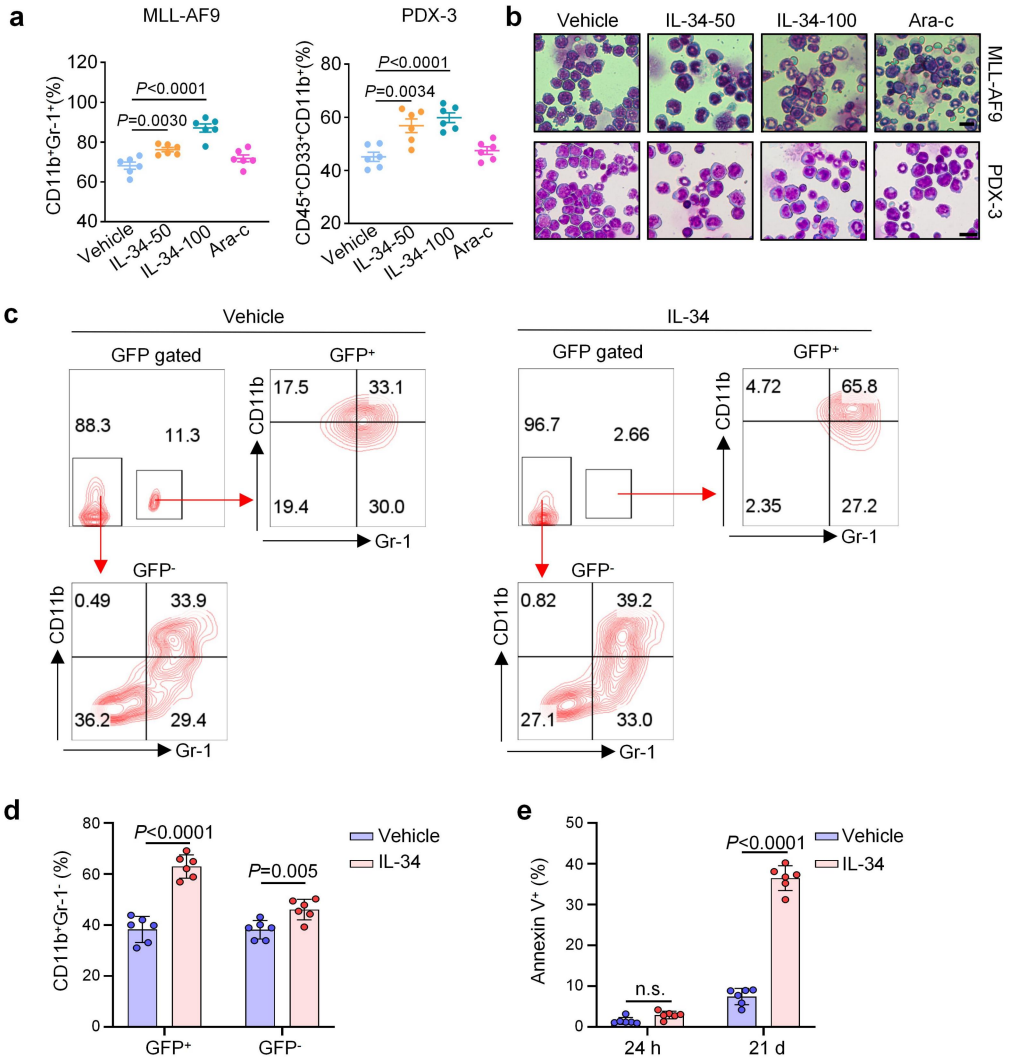

Fig. S3. IL-34 triggered leukemic cell differentiation *in vivo* (see also Fig. 2).

a, Flow cytometry analyses of mature myeloid cells in BM of mice treated with vehicle, IL-34, or Ara-C (n = 6). Populations are gated on GFP^+ cells (left) and $CD45^+CD33^+$ cells (right).

b, Representative Wright-Giemsa-stained cytospins of BM cells from IL-34-treated mice showing signs of granulocytic differentiation. Scale bars, 20 μm.

c, Flow cytometry gating strategy to analyze $CD11b^+Gr\text{-}1^+$ populations gated on GFP^+ or GFP^- cells from representative mice treated with vehicle or IL-34.

d, Flow cytometry analysis of $CD11b^+Gr\text{-}1^+$ populations gated on GFP^+ or GFP^- cells from representative mice treated with vehicle or IL-34 (n = 6).

e, Quantification of apoptosis of GFP^+ and GFP^- leukemia cells 24 h and 21 days

post-transplant (n = 6). Experiments were conducted 3–5 times for validation.

Statistical significance was calculated by one-way ANOVA with Turkey's multiple comparison test.

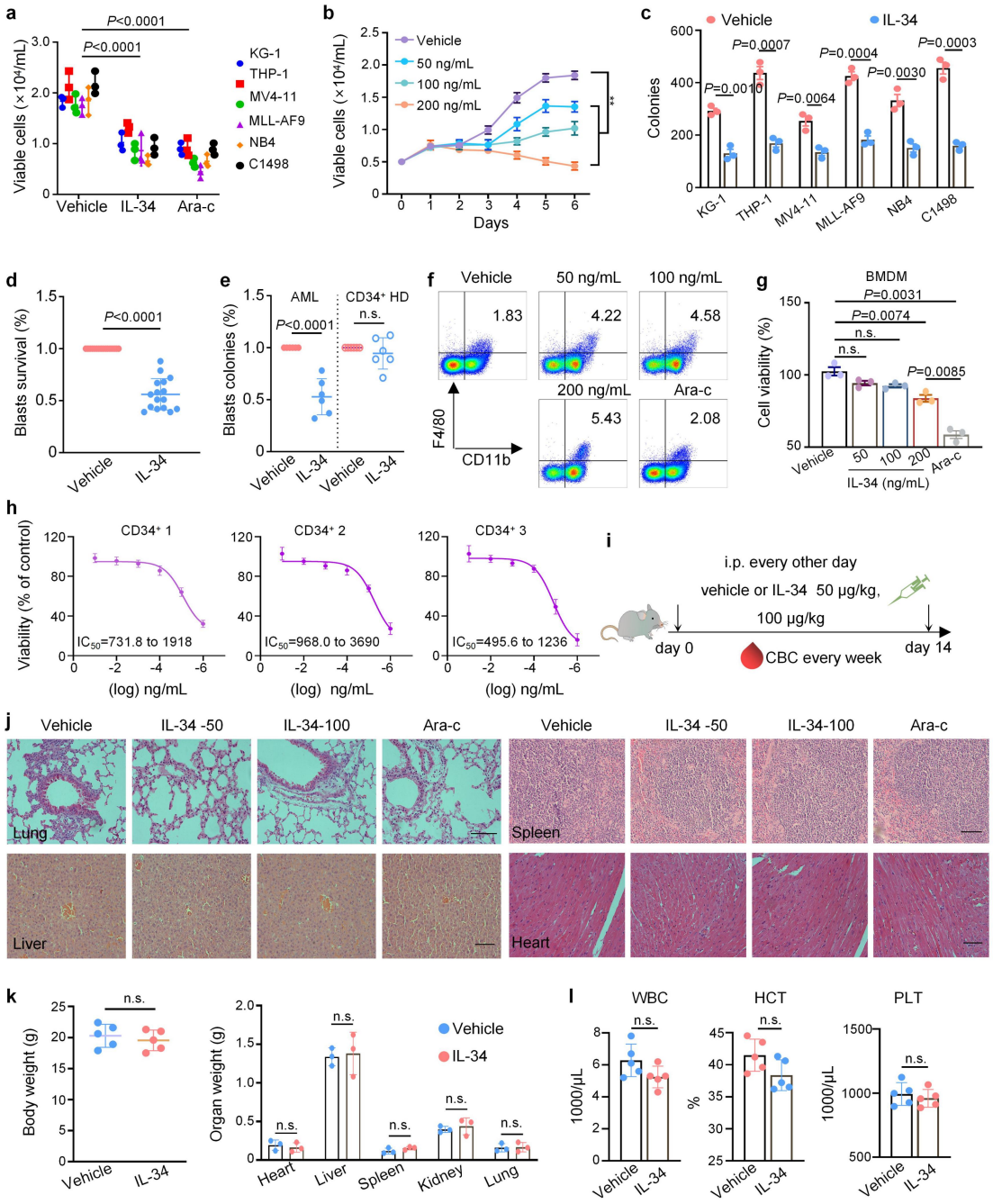

Fig. S4. IL-34 suppressed proliferation and induced differentiation of AML cells.

a, Cell viability of different AML cell lines treated with vehicle, Ara-C, or IL-34 (100 ng/mL).

b, Cell viability of C1498 cells treated with increasing doses of IL-34 (n = 3).

c, Colony formation of different AML cell lines treated with vehicle or IL-34 (100 ng/mL).

d, The relative number of $CD45^{dim}$ blasts after incubation with vehicle or 100 ng/mL rhIIL-34 of 17 primary AML cases.

e, Colony forming unit (CFU) assay using $CD34^+$ cells from AML patients and healthy donors (HD) treated with vehicle or IL-34 (n = 6).

f, $CD11b^+F4/80^+$ flow cytometry of BMDMs *in vitro* after differentiation induction by IL-34.

g, Cell viability of BMDMs treated with IL-34 or Ara-C for 72 h (n = 3).

h, Cell viability analysis of three human BM $CD34^+$ cells, treated with or without IL-34 for 72 h (n = 3).

i, Experimental design. The C57BL/6J mice (n = 5) were treated by intraperitoneal injection (i.p.) every other day with 50 and 100 μg/kg murine IL-34, respectively, for 14 days.

j, H&E staining of lung, liver, spleen, and heart tissues from vehicle- and IL-34- (100 μg/kg) treated C57BL/6J mice after dosing every other day for 14 days. Scale bars, 100 μm.

k, Body and organ weights of C57BL/6J mice (n = 5) treated with vehicle or IL-34 at 100 μg/kg every other day for 14 days. Weights were recorded at day 15.

l, Complete blood counts of mice in **i** (n = 5). Dosing every other day resulted in no anemia or thrombocytopenia.

The *P* values were calculated using a 2-tailed, unpaired Student *t* test.

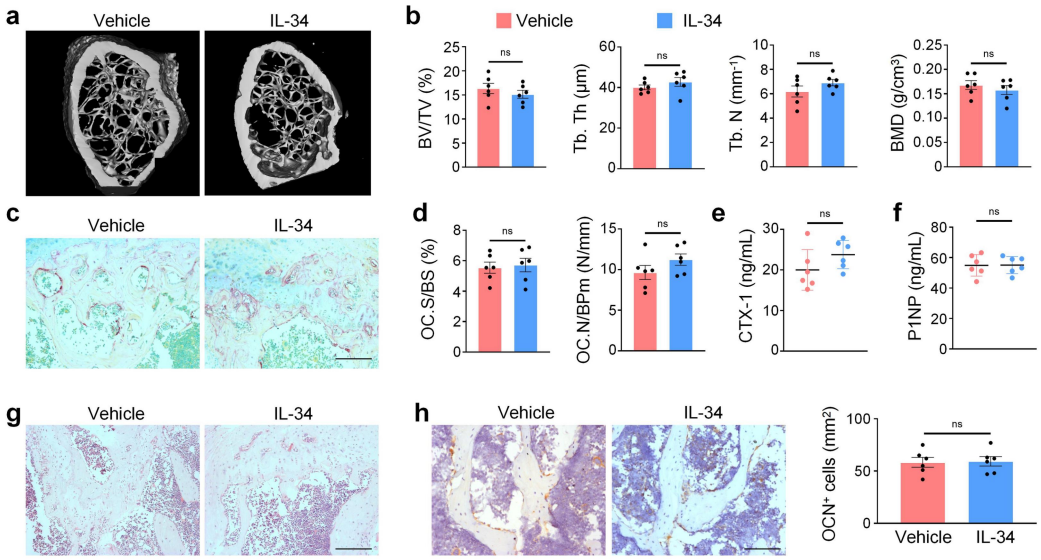

Fig. S5. IL-34 administration did not affect the osteoclast activity and bone morphology *in vivo*.

a, Three-dimensional μ-CT images of cortical bone of distal femurs isolated from the mice treated with IL-34 or vehicle (n = 6).

b, Quantitative analysis of the BV/TV, Tb.Th,Tb.N, and BMD (n = 6).

c, Osteoclast formation in bone. Tibial sections were subjected to tartrate-resistant acid phosphatase (TRAP) staining. Scale bars, 100 μm.

d, Quantitative analyses of the osteoclast surface/bone surface (Oc.S/BS) and osteoclast number/bone perimeter (Oc.N/BPm).

e, Serum levels of CTX-1 (n = 6).

f, Serum levels of P1NP (n = 6).

g, H&E staining images of distal femurs. Scale bars, 100 μm.

h, Representative OCN IHC images of distal femurs and relative quantitative analysis (n = 6). Scale bars, 100 μm.

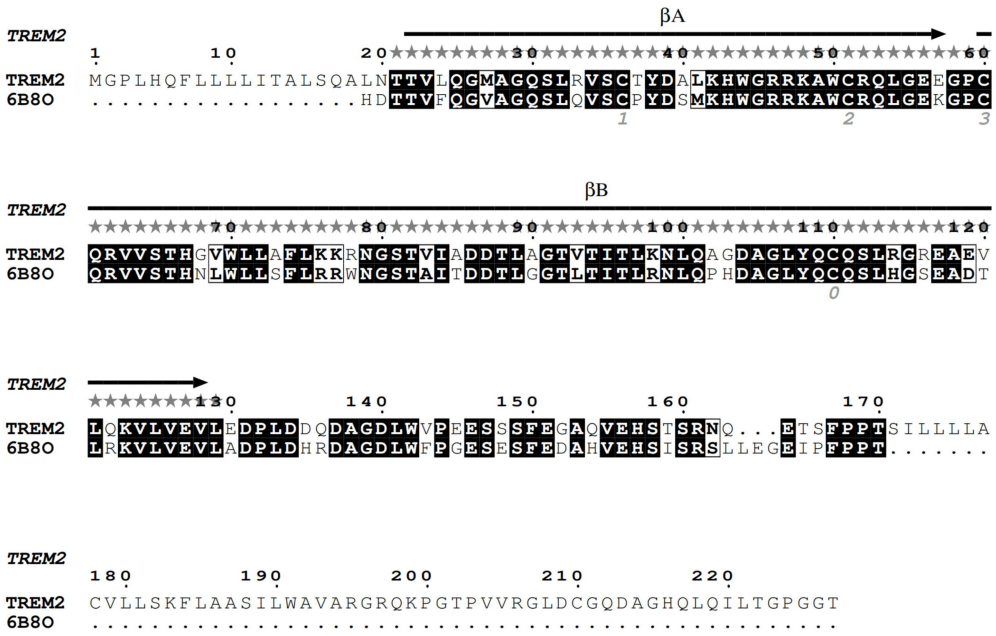

Fig. S6. The structure-based sequence comparison between TREM2 and the template structure. The mismatched residues are displayed with fade, and the sequence corresponding to alpha-helix and beta-strand regions are marked with black color.

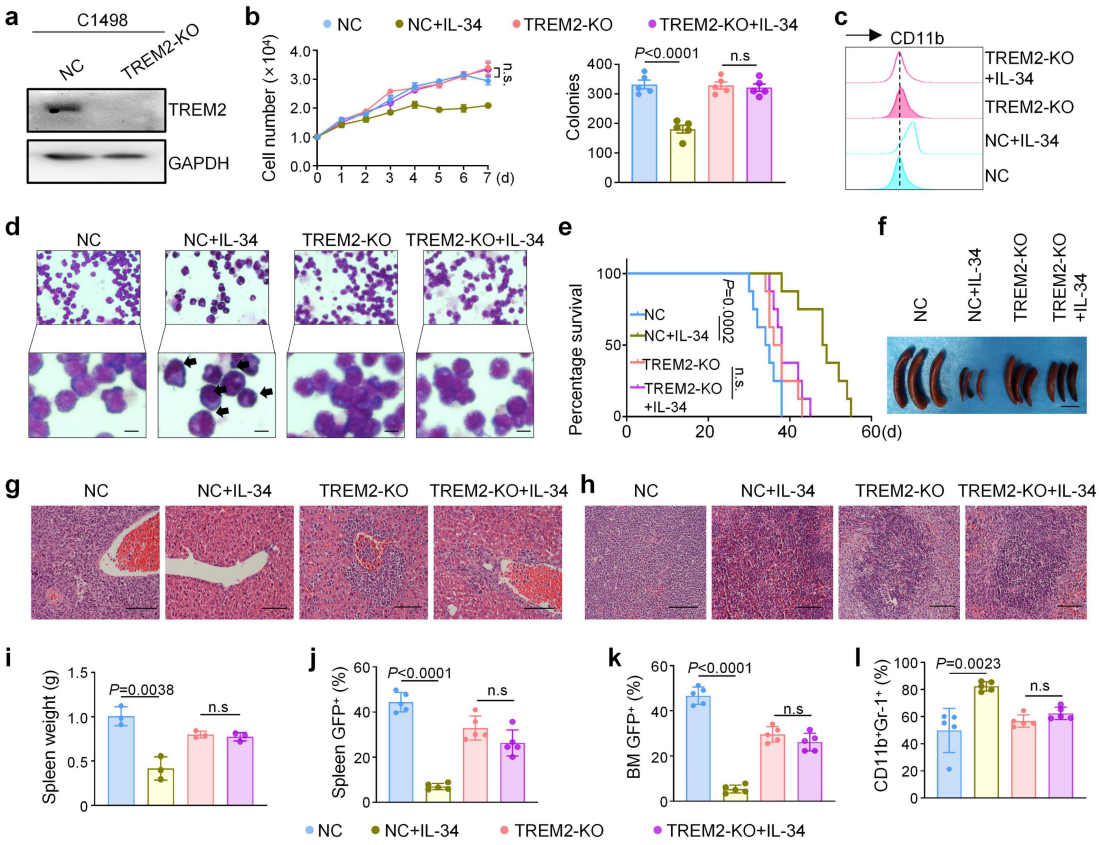

Fig. S7. IL-34 induced AML cell differentiation and prevented AML progression via TREM2 (see also Fig. 5).

a, Western blots confirming KO of TREM2 by CRISPR/Cas9 editing in C1498 cells.

b, Growth curves (left) and colony-forming assays (right) of C1498-TREM2-KO and C1498-NC cells after treatment with IL-34 (100 ng/mL) at the indicated time points (n = 5).

c, Flow cytometry analysis of CD11b expression in C1498-TREM2-KO and C1498-NC cells following IL-34 treatment.

d, Representative Giemsa staining images showing the morphology of C1498-TREM2-KO and C1498-NC cells following IL-34 treatment. Arrows highlight distinct morphology indicative of differentiation. Scale bars, 10 μm.

e, Kaplan–Meier survival curves of mice transplanted with C1498-NC or C1498-TREM2-KO cells treated with IL-34. Statistical assessment by log-rank test (n = 8).

f, Spleen appearance (n = 3). Scale bar, 1 cm.

g–h, H&E staining of the liver (g) and spleen (h) from C1498-NC or

C1498-TREM2-KO-engrafted mice treated with vehicle or IL-34 at day 28. Scale bars, 100 μm.

i, Spleen weights of mice receiving C1498-NC or C1498-TREM2-KO cells treated with or without IL-34 (n = 3).

j, Percentage of GFP^+ leukemic cells in spleen in mice engrafted with C1498-NC or C1498-TREM2-KO cells, followed by *in vivo* IL-34 treatment (n = 5).

k, Percentage of GFP^+ leukemic cells in BM in mice engrafted with C1498-NC or C1498-TREM2-KO cells, followed by *in vivo* IL-34 treatment (n = 5).

l, Flow cytometry plots depicting the percentage of $CD11b^+Gr\text{-}1^+$ cells in BM of C1498-NC or C1498-TREM2-KO-engrafted mice (n = 5).

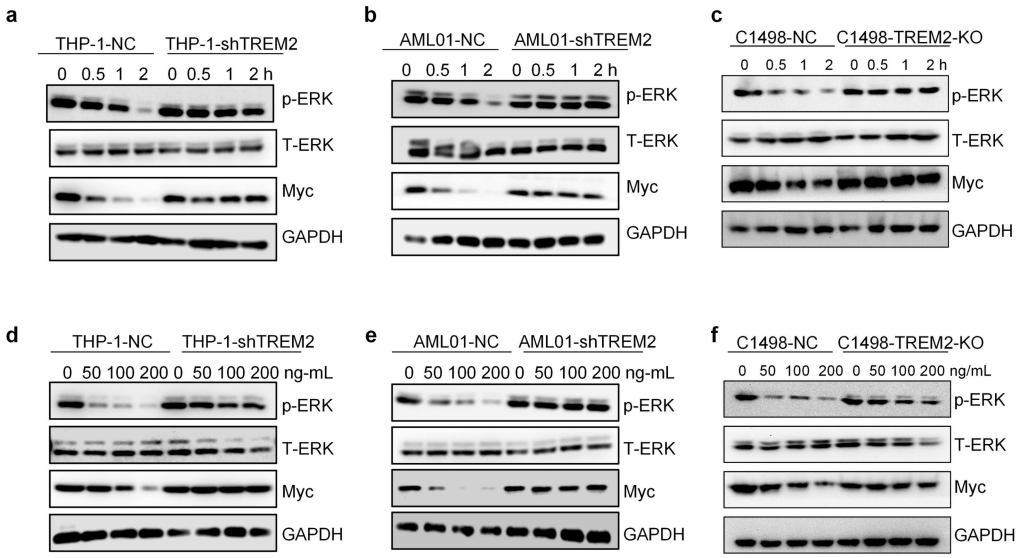

Fig. S8. IL-34–TREM2 rapidly inactivated ERK1/2 to induce AML cell differentiation (see also Fig. 6).

a–c, Western blot analysis of ERK1/2 protein/phosphorylation and Myc protein in THP-1-NC, THP-1-shTREM2 (**d**), AML01-NC, AML01-shTREM2 (**e**), C1498-NC, and C1498-TREM2-KO cells (**f**) treated with IL-34 (100 ng/mL) at the indicated time points (0, 0.5, 1, and 2 h).

d–f, Western blot analysis of ERK1/2 protein/phosphorylation and Myc protein in THP-1-NC, THP-1-shTREM2 (**a**), AML01-NC, AML01-shTREM2 (**b**), C1498-NC, and C1498-TREM2-KO cells (**c**) treated with IL-34 at the indicated concentrations (0, 50, 100, and 200 ng/mL) for 24 h.

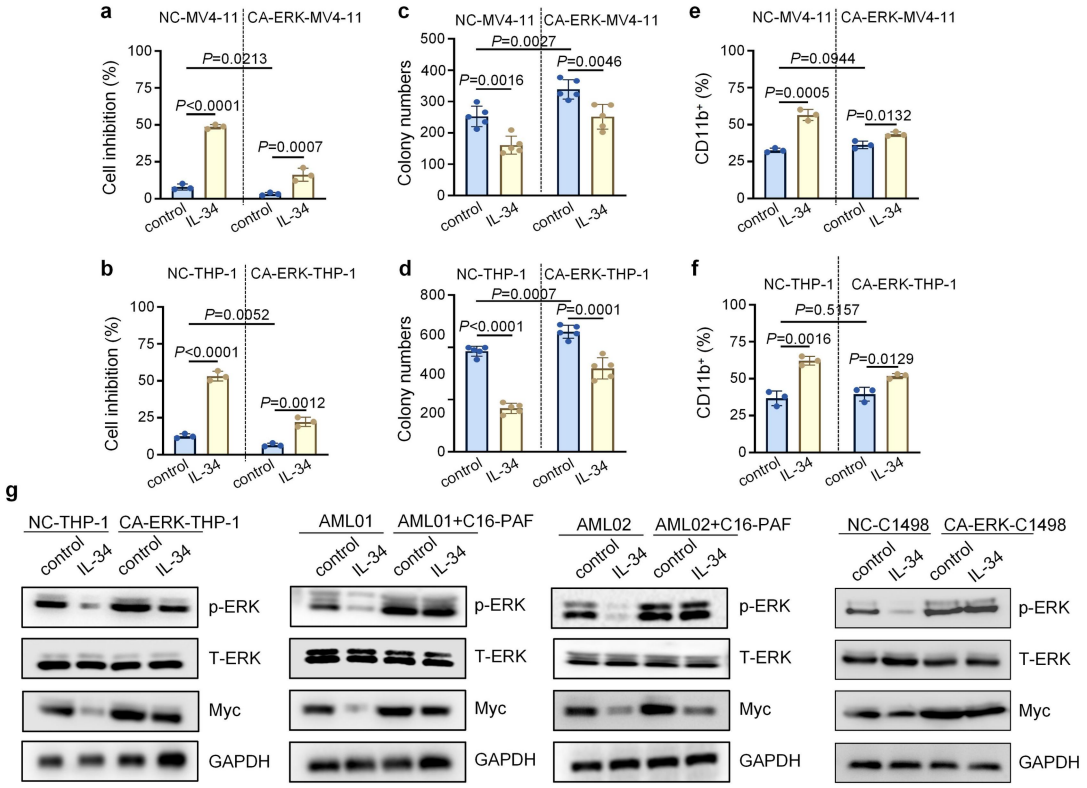

Fig. S9. IL-34–TREM2 inactivated ERK1/2 to induce AML cell differentiation (see also Fig. 6).

a–f, Overexpression of phosphorylated-ERK1/2 reversed the effects of IL-34 on MV4-11 and THP-1 cell growth (**a, b**), colonies (**c, d**), and differentiation (**e**, **f**). Mean ± SD (n = 3). Unpaired *t*-test.

g, Western blots demonstrating overexpression of phosphorylated-ERK1/2 in MV4-11, THP-1, and primary human AML cells and resultant changes in Myc protein level in response to IL-34 treatment.

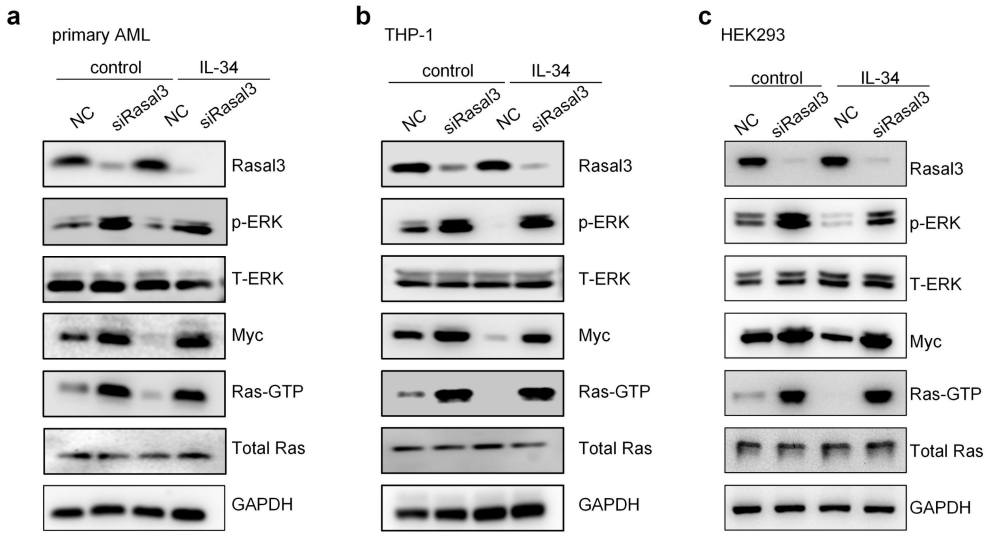

Fig. S10. IL-34–TREM2 rapidly inactivated ERK1/2 partially through phosphorylation of Rasal3 (see also Fig. 6).

Western blots demonstrating knockdown of Rasal3 expression in primary AML cells (**a**), THP-1 (**b**), and HEK293 (**c**) cells and resultant changes in activated Ras GTPase in response to IL-34 treatment.

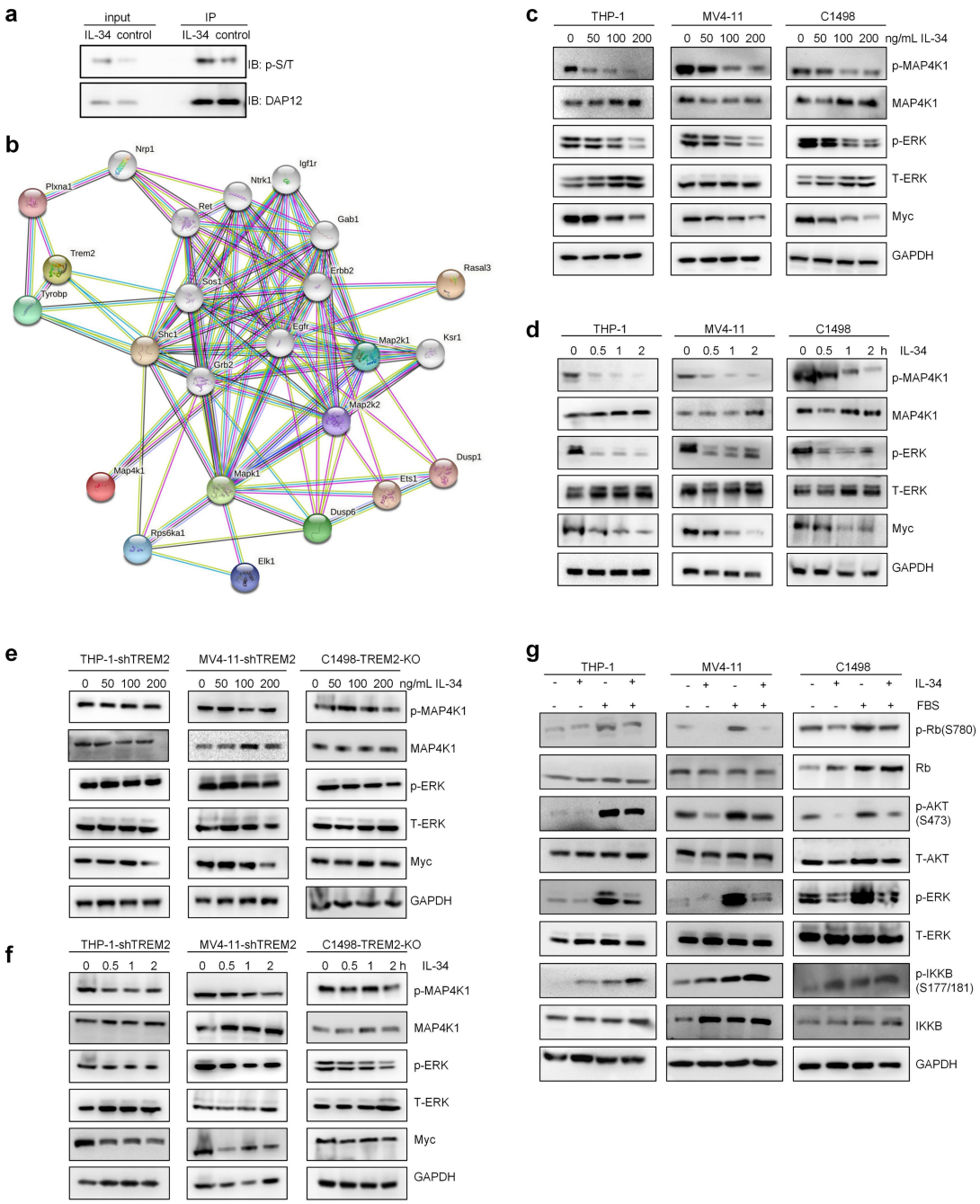

Fig. S11. IL-34 suppressed phosphorylation of MAP4K1, ERK1/2, and Myc signaling.

a, Co-immunoprecipitation analysis using the antibody against DAP12 followed by western blot analysis using antibodies against phosphorylated Thr/Ser in C1498 cells treated with IL-34.

b, Psychophysiological interactions (PPI) analysis of global quantitative phosphoproteomic data.

c, Western blot analysis of indicated AML cells (THP-1, MV4-11, and C1498) treated

with indicated concentrations (0, 50, 100, and 200 ng/mL) of IL-34 for 24 h. GAPDH, loading control.

d, Western blot analysis of indicated AML cells (THP-1, MV4-11, and C1498) treated at indicated time points (0, 0.5, 1, and 2 h) with IL-34 (100 ng/mL). GAPDH, loading control.

e, Western blot analysis of indicated AML cells transfected with shRNA or KO lentiviruses (THP-1-shTREM2, MV4-11-shTREM2, and C1498-TREM2-KO) treated with indicated concentrations (0, 50, 100 and 200 ng/mL) of IL-34. GAPDH, loading control.

f, Western blot analysis of indicated AML cells treated for indicated time points (0, 0.5, 1, and 2 h) with IL-34 after knockdown or knockout of TREM2. GAPDH, loading control.

g, Representative western blots of Rb, AKT, ERK1/2, and IKK protein/phosphorylation levels in THP-1, MV4-11, and C1498 cells treated with IL-34 (100 ng/mL) or 10% FBS for 30 min. Western blot has been repeated at least three times.

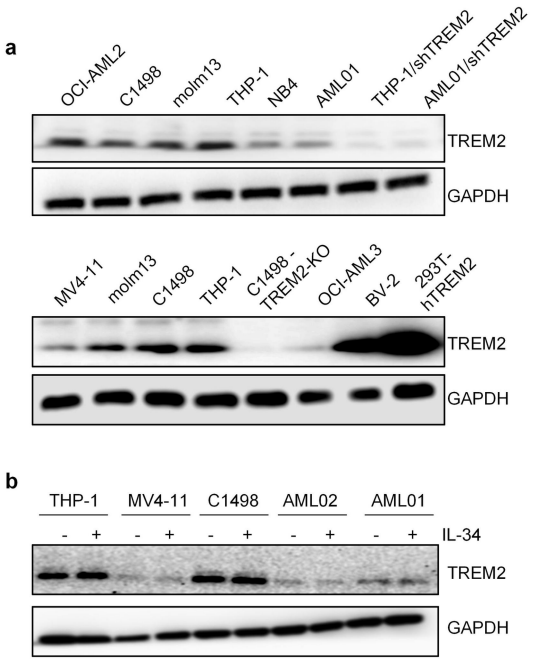

Fig. S12 in revision. IL-34 did not alter the expression levels of TREM2.

a, Western blot analysis of TREM2 protein levels in AML cell lines, negative controls (THP-1/shTREM2 and AML01/shTREM2 cells), and positive controls (293T-hTREM2, 293T cells transfected with a construct expressing GST-tagged full-length human TREM2 protein and BV-2 cells).

b, Western blot analysis of TREM2 protein levels in response to IL-34.

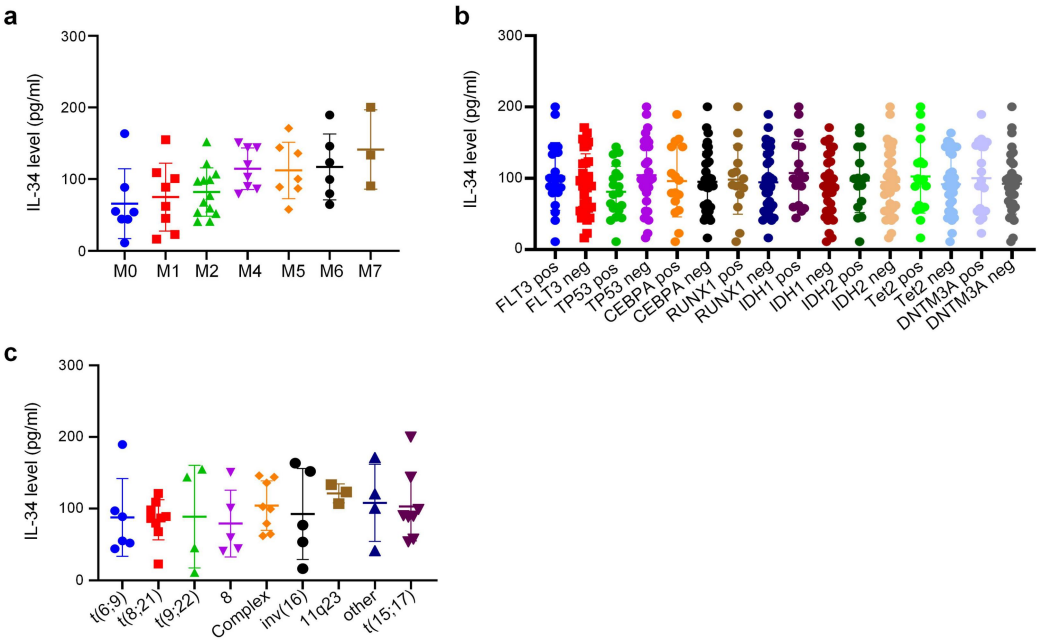

Fig. S13. **IL-34 correlated with the maturity stage of AML cells.**

a, Levels of IL-34 in M0–M7 defined FAB classified AML cases.

b, The expression patterns of IL-34 serum levels in AML patients with different molecular aberrancies.

c, The expression patterns of IL-34 serum levels in AML patients with different cytogenetics.

.